PRACTICAL IMPLEMENTATION OF INSTANTANEOUS FREQUENCY MASS SPECTROMETRY

Sasha Smith[1], *Steven Sandoval*[1*], *Tanner Schaub*[2], *and Phillip L. De Leon*[1,3]

New Mexico State University
[1]Klipsch School of Electrical and Computer Engineering
[2]Office of the Vice President for Research
Las Cruces, New Mexico, U.S.A.

[3]University of Colorado Denver
Department of Electrical Engineering
Denver, Colorado, U.S.A.

{sashamae,spsandov,tschaub}@nmsu.edu and Phillip.DeLeon@ucdenver.edu

ABSTRACT

We demonstrate instantaneous frequency (IF) mass spectrometry (MS) for the analysis of ion signals collected by image charge detection. We illustrate IFMS for ion motion frequency estimation based on instantaneous spectral analysis for the first time with experimentally-collected ion signals. This approach allows the observation of time-varying frequency estimates in contrast to typical Fourier transform mass spectrometry (FTMS) which provides constant frequency estimates of spectral peaks. We illustrate this approach for signals of quadrupole-selected ions collected with an Orbitrap mass spectrometer. We observe time-varying frequency phenomena in all ion transient signals and note an interesting observation with regard to the isotopologue signals of caffeine. While the source of this time-varying phenomena has yet to be determined, to the best of our knowledge, this is the first observation of such behavior in an Orbitrap system utilizing IF analysis. Finally, we provide deviation statistics of the IF from the FFT estimate using our entire dataset and demonstrate that the time-averaged IF is in general agreement with the frequency estimates provided by the FFT.

Index Terms— Mass spectroscopy, Spectral analysis, Fourier transforms, Adaptive signal processing

1. INTRODUCTION

Mass spectrometry (MS) provides precise data from systems as diverse as constrained industrial environments to open Earth systems (e.g. soils, waterways, oceans), as well as tissues and the cellular structures of organisms. Among the MS configurations are techniques that rely on image charge detection and Fourier transform-based signal processing such as Fourier transform mass spectrometry (FTMS). Of these, Fourier transform ion cyclotron resonance (FT-ICR) mass spectrometer is the premier tool for description of the world's most complex mixtures [1,2] and the Orbitrap mass spectrometer is the most broadly distributed and applied of the high resolution MS systems [3].

Time-dependent frequency components have been predicted for FTMS ion signals for both Orbitrap and FT-ICR instruments [4–6]. A variety of mechanisms to explain the frequency variation have been proposed [7–9]. A description of time-dependent instantaneous frequency (IF) has been proposed to describe ion motion and spectral generation in FTMS [10]. The benefit of instantaneous analysis may be in additional insight into numerous experimental processes, e.g. RF excitation, transient decay, frequency shifting, and frequency to mass-to-charge ratio (m/z) calibration, where additional improvements may be achieved [10].

The overarching goal of this work is to observe time-varying frequency phenomena in MS transient signals. To that end, we introduce instantaneous frequency mass spectrometry (IFMS) as a new means of analyzing mass spectrometer signal transients. Traditional Fourier-based methods, such as FTMS, utilize the FFT to produce high-precision results with the use of relatively long signal observations. On the other hand, the precision of instantaneous spectral analysis (ISA) [11] and adaptive mode decompositions (AMDs) [12, 13, 13] does not depend on the signal length, but rather the sampling rate. Thus, we propose an end-to-end method in which IF estimates are obtained via AMD followed by ISA. Although prior work [10] has been conducted in simulation, to our knowledge this is a first demonstration of an actual implementation of IFMS using experimental data. By enabling the observation of time-varying ion behavior, our proposed end-to-end method has the potential to provide insight related to ion motion or could lead to efforts to improve state-of-the-art instrumentation.

The remainder of this paper is organized as follows. In Section 2, we introduce our dataset and proposed end-to-end signal processing method for IF estimation for MS, using an AMD and ISA. Section 3 provides an illustrative example using caffeine ion signals, which includes the IF estimates for the isotopes. Additionally, we provide and discuss summarizing statistics which compare values from the IF with those from the FFT. Finally, in Section 4 we conclude the article.

2. INSTANTANEOUS SPECTRAL ANALYSIS OF MASS SPECTROMETER SIGNAL TRANSIENTS

In this section, we describe the data collection environment and the proposed end-to-end method for ISA of the signal transients. This method includes a preprocessing stage, estimation of initialization parameters for variational nonlinear chirp mode decomposition (VNCMD), signal decomposition via VNCMD, and AM-FM demodulation which results in a sequence of instantaneous amplitude (IA) and IF estimates for each signal component. Fig. 1 shows

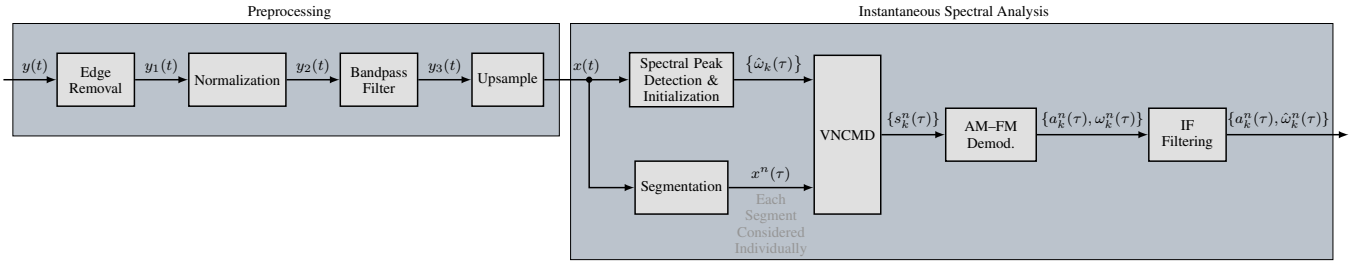

Fig. 1. Block diagram of the proposed end-to-end method for ISA of the signal transients. A transient signal $y(t)$ is pre-processed with edge removal, normalization, bandpass filtering, and upsampling. The preprocessed signal $x(t)$ is then utilized to estimate parameters for the initialization of the VNCMD algorithm, $\{\hat{\omega}_k(\tau)\}$, and segmented into a set of 201 sample segments, $x^n(\tau)$. Via VNCMD, each segment $x^n(\tau)$ is then decomposed into (real) AM–FM components $\{s_k^n(\tau)\}$ which are then demodulated into instantaneous frequency estimates $\{a_k^n(\tau), \omega_k^n(\tau)\}$. These frequency estimates are then filtered in order to attenuate the numerical effects, yielding $\{a_k^n(\tau), \hat{\omega}_k^n(\tau)\}$.

the block diagram where $y(t)$ denotes a signal transient to be analyzed. A series of preprocessing steps are first performed on the transient, including edge removal, normalization, bandpass filtering, and upsampling. This yields the signals $y_1(t)$, $y_2(t)$, $y_3(t)$ and $x(t)$, respectively as shown in the figure. In the upper branch of the figure, the preprocessed signal $x(t)$ is then used to estimate parameters for the initialization of the VNCMD algorithm, $\{\hat{\omega}_k^n(\tau)\}$ where n is the index for the signal segment, k is the index for the component, and τ is the segment time index. In the lower branch of the figure, the preprocessed signal $x(t)$ is segmented into a set of 201 sample segments, $\{x^n(\tau)\}$. Each segment $x^n(\tau)$ is then decomposed into (real) AM–FM components $\{s_k^n(\tau)\}$ via VNCMD which are then demodulated into IA, IF estimates $\{a_k^n(\tau), \omega_k^n(\tau)\}$. These IF estimates are then filtered in order to mitigate the numerical effects, yielding $\{a_k^n(\tau), \bar{\omega}_k^n(\tau)\}$. In the following sections, each of the steps is discussed in more detail.

2.1. Data

The liquid solution used for data collection, Pierce™ FlexMix™ Calibration Solution, consists of several chemical standards which are listed in [14]. Explicitly, we selected the dataset for this investigation to include caffeine, a peptide (MRFA), and an Ultramark (UM1621) polymer that consists of a series of polymer molecules with masses that are 100 Da apart [15].

We collected time-domain signals from a *Thermo Fisher Scientific Orbitrap Fusion* [16] mass spectrometer with stand-alone signal collection/processing electronics *SpectroSwiss PXI FTMS Booster* [17,18] located at the New Mexico State University, Chemical Analysis and Instrumentation Laboratory (CAIL). Each data transient was collected with sampling frequency $f_s = 3.90625$ MHz and consists of approximately 0.78 - 1.21 s of data, where slight variation in collected length was an unintended consequence of the available experimental triggering set-up. Table 1 lists all of the ions considered in the Calibration Solution along with their corresponding m/z ratios.

2.2. Signal Preprocessing

As shown in Fig. 1, the signal preprocessing consists of edge removal, normalization, filtering, and upsampling.

2.2.1. Edge Removal

The raw transient signal $y(t)$ contains artifacts that are introduced by the instrumentation at the start and end of the transient recording.

Table 1. The frequency bands utilized to capture critical regions of the spectrum for the molecules under consideration were separated into four non-overlapping bands. Caffeine and MRFA each have unique filters because of their spectral isolation, while UM1022, UM1121, UM1221, UM1321 share a single filter range and UM1421, UM1521, UM1621, UM1721 share another single filter due to close spectral proximity.

Filter	**Freq (MHz)**	**Nominal m/z**	**Ions(s)**
BPF 1	0.825 - 1.0500	195	caffeine
BPF 2	0.634 - 0.6390	524	MRFA
BPF 3	0.400 - 0.5000	1022, 1122, 1222, 1322	UM1022-UM1322
BPF 4	0.340 - 0.3865	1422, 1522, 1622, 1722	UM1422-UM1722

Therefore, we remove the artifacts by trimming 800 samples at the start and 11,700 samples from the end, resulting in the signal $y_1(t)$.

2.2.2. Normalization

For convenience, the trimmed signal $y_1(t)$ is amplitude normalized to have values ranging between $+1$ and -1, resulting in $y_2(t)$.

2.2.3. Bandpass Filtering

Experimentally, we found that working with the entire broadband spectral range (100-2000 m/z) led to inconsistent decomposition. Therefore, we utilized a filterbank to separate the spectrum into four non-overlapping frequency bands. The filters have center frequencies and bandwidths designed to capture critical regions of the spectrum for the molecules under consideration. However, the regions are not selected to favor any specific molecule, as would be in practice, given no prior information on the substance under analysis. Table 1 lists the frequency ranges of the filters as well as the ions which fall within each range. Later in this section, information on the UM ions used in the analysis will be provided. For implementation, we choose to use a Butterworth filter of order six and to prevent phase distortion, we filter the normalized signal $y_2(t)$ in both forward and reverse directions resulting in $y_3(t)$.

2.2.4. Upsample

When using Fourier-based analysis methods, satisfying the Nyquist-Shannon sampling criteria is sufficient to avoid aliasing effects [19]. However, accurate estimation of *IFs* via demodulation (e.g. using an FM discriminator) requires oversampling due to numerical differentiation [20]. Therefore, to have sufficient time-resolution to perform accurate instantaneous demodulation, the bandpass filtered signal $y_3(t)$ was upsampled by a factor of six, yielding the signal $x(t)$.

2.3. Instantaneous Spectral Analysis

ISA consists of two major steps: signal decomposition into AM–FM components and demodulation of the components. There are a wide variety of AMDs [12, 13, 13, 21, 22] that can be used to decompose a signal into a set of constituent signal components. For this work, we choose the VNCMD algorithm [23] because it allows the initialization of parameters which yields more accurate and consistent components than other AMDs we tried including empirical mode decomposition (EMD) and variational mode decomposition (VMD). For more information on ISA theory and implementation, we refer the reader to [11, 24, 25]. As shown in Fig. 1, the ISA for MS consists of spectral peak detection, segmentation, signal decomposition, AM–FM demodulation and IF filtering.

2.3.1. Spectral Peak Detection and Initialization

The VNCMD algorithm requires initial IF estimates in the form of a time-series for each of the signal components. These initial IF estimates were obtained via an FFT on $x(t)$ with spectral peak detection, resulting in the initialization parameters of the VNCMD algorithm $\{\hat{\omega}_k(\tau)\}$.

2.3.2. Segmentation

The signal $x(t)$ is segmented into intervals of length 201 samples (chosen for computational convenience) resulting in $\{x^n(\tau)\}$, where n denotes the interval index.

2.3.3. Signal Decomposition

Parameters for VNCMD as follows are bandwidth constraint $\alpha = 5 \times 10^{-12}$, convergence constraint $\beta = 0.5 \times 10^{-2}$, and noise variance $\sigma^2 = 0$ [13]. For each segment $x^n(\tau)$ VNCMD results in a set of signal components denoted $s_k^n(\tau)$ where k is the component index, n denotes the interval index, and $0 \leq \tau \leq 200$.

2.3.4. AM–FM Demodulation

Following decomposition, each AM–FM signal component segment $s_k^n(\tau)$ is assumed to consist of an intrinsic mode function [12] and is demodulated to yield IA, IF estimates $a_k^n(\tau)$, $\omega_k^n(\tau)$ using the demodulation algorithm given in [20].

2.3.5. IF Filtering

To alleviate some of the numerical errors introduced by the decomposition and demodulation steps, the IF estimates were smoothed resulting in $\hat{\omega}_k^n(\tau)$.

3. RESULTS AND DISCUSSION

Although the emphasis of this work is in developing an approach for IF estimation for transient analysis, it is important to compare the time-averaged IF estimate $\bar{\omega}_k$ to the FFT estimate ω_k^{FFT}. At the conclusion of the end-to-end method, we have $a_k^n(\tau), \hat{\omega}_k^n(\tau)$. We concatenate the IF segments, $\hat{\omega}_k^n(\tau)$, to form a single time-series

$$\hat{\omega}_k(t) = \left[\hat{\omega}_k^1(\tau), \hat{\omega}_k^2(\tau), \cdots, \hat{\omega}_k^N(\tau)\right]. \tag{1}$$

This process is repeated for each individual component, k. We define the estimation deviation as

$$\Delta = \left|\bar{\omega}_k - \omega_k^{\mathrm{FFT}}\right| \tag{2}$$

via the expectation operator $\mathbb{E}_t[\cdot]$

$$\bar{\omega}_k = \mathbb{E}_t\left[\hat{\omega}_k(t)\right]. \tag{3}$$

Table 2 gives the mean and standard deviation of the IF estimation deviations, i.e. $\bar{\Delta}$ and $\bar{\sigma}$, for the dataset.

We note in Table 2 that in general, $\bar{\Delta}$ is less than 1 Hz for the ion signals under examination with the exception of those signals at the band edges. IF-derived frequency estimates vary most markedly for caffeine ion signals, which are the ions with the lowest m/z and highest motional frequency of our test mixture. Note that the quadrupole ion selection window employed, 2 m/z, results in multiple isotopologues being present within the Orbitrap, and these ion ensembles interact during the measurement. Ion-ion interactions and/or other electric field imperfections that affect ion motion and frequency occur at higher rates for lighter ions and may account for the exaggerated variability of IF estimates across those signal segments which are temporally-separated.

In order to compute a range for the FFT frequency resolution, we consider the shortest and longest signal windows and the number of points in the FFT. The shortest signal window was for the caffeine ion signal which resulted in 18,213,498 samples while the longest signal window was for the UM1721 molecule which resulted in 28,394,010 samples. Therefore, the range of the FFT frequency resolution is 0.83–1.29 Hz. We find that in general, the average deviations are on the order of the FFT resolution and thus, the estimates provided from an average IF are in agreement with the FFT.

Of all the ions in Table 2, the caffeine ion signal exhibited the most deviation. Fig. 2 illustrates $\hat{\omega}_k(t)$ for components associated with caffeine ion signals, with each of the three components shown corresponding to a peak in the FFT magnitude spectrum shown in Fig. 3. For the convenience of the reader, we have superimposed a horizontal line in Fig. 2 at the numerical value of each peak in Fig. 3 corresponding to the FFT-based estimate for these ion signals. Fig. 2 shows unexpected periodic oscillation in the correspondent time series. We note that, although not shown, all molecules subjectively appear to have a deviation which is correlated across the isotopes although it may not be periodic. Further perturbation of the system in terms of ion number, observation period, and spectral composition are needed to determine the source of these frequency fluctuations and the patterns observed in Fig. 2. The IFMS process described here is uniquely suited to the study of such phenomena.

To the best of our knowledge, this is the first observation of such time-varying behavior through the use of IF analysis. We hypothesize that this variation could be attributed to either 1) ion behavior or 2) instrumentation artifacts, but determining the true source of this variation is beyond the scope of this work. While not fully understood, this observation may be of importance in advancing MS. If this observation is due to ion behavior, this work could potentially

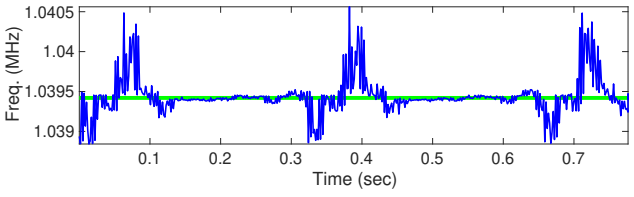

(a) $^{13}O_1C_7H_{10}N_4O_2$

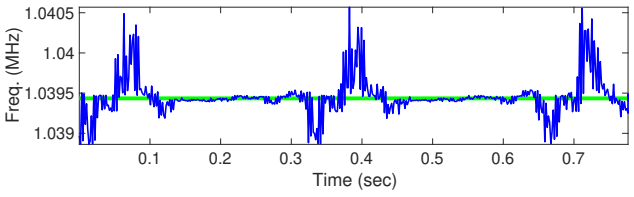

(b) $^{15}N_1C_7H_{10}N_3O_2$

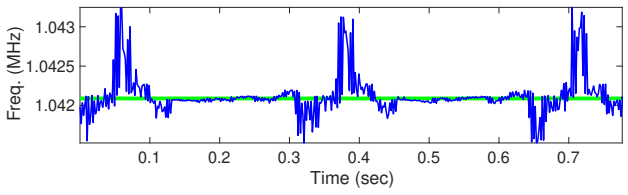

(c) $C_8H_{10}N_4O_2$

Fig. 2. Instantaneous frequency estimates (—) for three caffeine ions (a) ($^{13}O_1C_7H_{10}N_4O_2$) + [H+], (b) ($^{15}N_1C_7H_{10}N_3O_2$) + [H+], and (c) ($C_8H_{10}N_4O_2$) + [H+]. In each of the plots, we see consistent oscillations across the signal, however, there are sections (in between 0.15 seconds and 0.27 for example) which appear to be more constant near the FFT peak frequency (—).

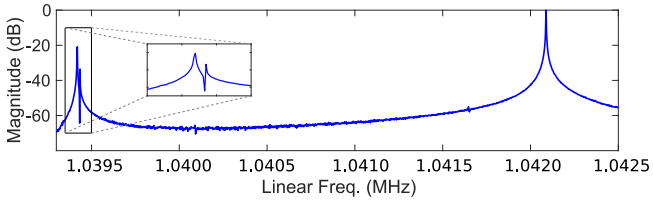

Fig. 3. Magnitude spectrum for caffeine showing three expected peaks at 1.03941959 MHz ($^{13}O_1C_7H_{10}N_4O_2$) + [H+], 1.03943493 MHz ($^{15}N_1C_7H_{10}N_3O_2$) + [H+], and 1.04208900 MHz ($C_8H_{10}N_4O_2$) + [H+].

provide more insight related to ion motion or if this observation is due to artifacts, this work could improve state-of-the-art instrumentation.

4. CONCLUSION

In this paper, we proposed an end-to-end method for IF estimation of MS signal transients using VNCMD and ISA. The resulting IF sequence enables the observation of time-varying frequency phenomena in a single transient. Using a Thermo Fisher Scientific Orbitrap Fusion with SpectroSwiss PXI FTMS Booster, we acquired MS signal transients for several molecules, performed ISA, and observed time-varying frequency phenomena in the transient, which to our knowledge, has not previously been observed. The most interesting time-varying frequency phenomena was observed in the caffeine sample. Although the source of the time-varying phenomena is currently unknown, we conjecture that it may be attributed to ion behavior or instrumentation artifacts. In addition, we provided deviation statistics of the IF from the FFT estimate and demonstrated that the time-averaged IF of each component of each molecule is in agreement with the frequency estimates provided by the FFT. Finally, by enabling the observation of time-varying ion behavior, our proposed end-to-end method has the potential to provide insight related to ion motion or could lead to efforts to improve state-of-the-art instrumentation. This ability to observe time-varying ion behavior during ion signal detection can inform study of ion cloud signal coalescence for ion packets with minimal m/z differences (i.e. peak coalescence), optimize the shapes for electrodes involved in ion trapping, excitation, and detection, and provide insight on optimum ion excitation and isolation waveforms for different trap geometries, and monitor the evolution of ion-ion interactions that perturb ion motion and limit signal resolution, for example.

Table 2. $\bar{\omega}_k^{\mathrm{FFT}}$ denotes the frequency estimate from the FFT averaged over the transient signals. The mean and standard deviation of the deviation.

Isotope	$\bar{\omega}_k^{\mathrm{FFT}}$ (Hz)	$\bar{\Delta}$ (Hz)	$\bar{\sigma}$ (Hz)
Caffeine–1	1,039,419.59	4.533	18.958
Caffeine–2	1,039,434.93	4.593	18.990
Caffeine–3	1,042,089.00	5.426	19.744
MRFA–1	634,485.38	0.583	2.498
MRFA–2	634,491.88	0.582	2.512
MRFA–3	635,091.08	0.588	2.523
MRFA–4	635,698.32	0.597	2.534
UM1022–1	454,856.31	0.068	1.068
UM1022–2	455,079.17	0.096	1.323
UM1022–3	455,302.57	0.076	1.098
UM1121–1	434,152.58	0.688	0.708
UM1121–2	434,346.45	0.705	0.718
UM1121–3	434,540.66	0.709	0.747
UM1221–1	416,040.87	0.633	0.644
UM1221–2	416,211.45	0.658	0.648
UM1221–3	416,382.33	0.661	0.653
UM1321–1	400,021.69	0.617	0.773
UM1321–2	400,173.40	0.608	0.781
UM1321–3	400,325.29	0.612	0.786
UM1421–1	385,151.07	0.641	0.487
UM1421–2	385,856.94	0.570	0.508
UM1421–3	385,993.13	0.565	0.514
UM1521–1	372,852.24	0.618	0.388
UM1521–2	372,974.97	0.544	0.388
UM1521–3	373,097.78	0.546	0.403
UM1621–1	361,190.99	0.552	0.380
UM1621–2	361,302.59	0.531	0.389
UM1621–3	361,414.14	0.532	0.390
UM1721–1	350,559.53	1.655	1.272
UM1721–2	350,661.64	1.762	1.304
UM1721–3	350,763.77	1.750	1.308

5. ACKNOWLEDGEMENTS

The authors wish to thank to Maha Abutokaikah of the Research Cores Program at New Mexico State University for assistance with data collection and Yury O. Tsybin of École Polytechnique Fédérale de Lausanne (EPFL) for reviewing early drafts of this manuscript.

6. REFERENCES

[1] D. F. Smith, D. C. Podgorski, R. P. Rodgers, G. T. Blakney, and C. L. Hendrickson, "21 Tesla FT-ICR mass spectrometer for ultrahigh-resolution analysis of complex organic mixtures," *Anal. Chem.*, vol. 90, no. 3, pp. 2041–2047, 2018.

[2] M. L. Chacón-Patiño, M. R. Gray, C. Rüger, D. F. Smith, T. J. Glattke, S. F. Niles, A. Neumann, C. R. Weisbrod, A. Yen, A. M. McKenna, P. Giusti, B. Bouyssiere, C. Barrère-Mangote, H. Yarranton, C. L. Hendrickson, A. G. Marshall, and R. P. Rodgers, "Lessons learned from a decade-long assessment of asphaltenes by ultrahigh-resolution mass spectrometry and implications for complex mixture analysis," *Energy & Fuels*, vol. 35, no. 20, pp. 16 335–16 376, 2021.

[3] S. Eliuk and A. Makarov, "Evolution of orbitrap mass spectrometry instrumentation," *Annu. Rev. Anal. Chem.*, vol. 8, no. 1, pp. 61–80, 2015.

[4] K. Aizikov and P. B. O'Connor, "Use of the filter diagonalization method in the study of space charge related frequency modulation in Fourier transform ion cyclotron resonance mass spectrometry," *J. Am. Soc. Mass Spectrom.*, vol. 17, no. 6, pp. 836–843, 2006.

[5] T. Aushev, A. N. Kozhinov, and Y. O. Tsybin, "Least-squares fitting of time-domain signals for Fourier transform mass spectrometry," *J. Am. Soc. Mass Spectrom.*, vol. 25, no. 7, p. 1263–1273, 2014.

[6] F. E. Leach, A. Kharchenko, G. Vladimirov, K. Aizikov, P. B. O'Connor, E. Nikolaev, R. M. A. Heeren, and I. J. Amster, "Analysis of phase dependent frequency shifts in simulated FTMS transients using the filter diagonalization method," *Int. J. Mass Spectrom.*, vol. 325-327, pp. 19–24, 2012.

[7] S. M. Miladinović, A. N. Kozhinov, O. Y. Tsybin, and Y. O. Tsybin, "Sidebands in Fourier transform ion cyclotron resonance mass spectra," *Int. J. Mass Spectrom.*, vol. 325-327, pp. 10–18, 2012.

[8] R. L. Wong and I. J. Amster, "Experimental evidence for space-charge effects between ions of the same mass-to-charge in fourier-transform ion cyclotron resonance mass spectrometry," *Int. J. Mass Spectrom.*, vol. 265, no. 2-3, pp. 99–105, 2007.

[9] C. Hendrickson, S. Beu, G. Blakney, and A. Marshall, "SIMION modeling of ion image charge detection in Fourier transform ion cyclotron resonance mass spectrometry," *Int. J. Mass Spectrom.*, vol. 283, pp. 100–104, 2009.

[10] O. Y. Tsybin and Y. O. Tsybin, "Time-dependent frequency of ion motion in Fourier transform mass spectrometry," *Int. J. Mass Spectrom.*, vol. 376, pp. 75–84, 2015.

[11] S. Sandoval and P. L. De Leon, "The instantaneous spectrum: A general framework for time-frequency analysis," *IEEE Trans. Signal Process.*, vol. 66, pp. 5679–5693, Nov 2018.

[12] N. E. Huang, Z. Shen, S. R. Long, M. C. Wu, H. H. Shih, Q. Zheng, N. C. Yen, C. C. Tung, and H. H. Liu, "The empirical mode decomposition and the hilbert spectrum for nonlinear and non-stationary time series analysis," *Proc. R. Soc. London Ser. A*, vol. 454, no. 1971, pp. 903–995, Mar. 1998.

[13] K. Dragomiretskiy and D. Zosso, "Variational mode decomposition," *IEEE Trans. Signal Process.*, vol. 62, no. 3, pp. 531–544, 2014.

[14] Thermo Fisher Scientific. Pierce™ FlexMix™ Calibration Solution. Accessed: January 11, 2022. [Online]. Available: https://www.thermofisher.com/order/catalog/product/A39239

[15] Alfa Aesar by Thermo Fisher Scientific. L16698 ultramark® 1621, mass spec std. Accessed: May 10, 2022. [Online]. Available: https://www.alfa.com/en/catalog/L16698/

[16] Thermo Fisher Scientific. Orbitrap Fusion™ Lumos™ Tribrid™ Mass Spectrometer. Accessed: May 10, 2022. [Online]. Available: https://www.thermofisher.com/order/catalog/product/IQLAAEGAAPFADBMBHQ?SID=srch-srp-IQLAAEGAAPFADBMBHQ

[17] J. R. Bills, K. O. Nagornov, A. N. Kozhinov, T. J. Williams, Y. O. Tsybin, and R. K. Marcus, "Improved uranium isotope ratio analysis in liquid sampling–atmospheric pressure glow discharge/orbitrap ftms coupling through the use of an external data acquisition system," *J. Am. Soc. Mass Spectrom.*, vol. 32, no. 5, pp. 1224–1236, 2021. [Online]. Available: https://doi.org/10.1021/jasms.1c00051

[18] K. O. Nagornov, M. Zennegg, A. N. Kozhinov, Y. O. Tsybin, and D. Bleiner, "Trace-level persistent organic pollutant analysis with gas-chromatography orbitrap mass spectrometry—enhanced performance by complementary acquisition and processing of time-domain data," *J. Am. Soc. Mass Spectrom.*, vol. 31, no. 2, pp. 257–266, 2020. [Online]. Available: https://doi.org/10.1021/jasms.9b00032

[19] A. V. Oppenheim, A. Willsky, and S. H. Nawab, *Signals and Systems*, 2nd ed. Prentice Hall, 1997.

[20] S. Sandoval and P. L. De Leon, "Advances in Empirical Mode Decomposition for Computing Instantaneous Amplitudes and Instantaneous Frequencies," in *Proc. IEEE Int. Conf. Acoust. Speech Signal Process.* IEEE, Mar. 2017, pp. 4311–4315.

[21] P. Flandrin, *Explorations in Time-Frequency Analysis*, 1st ed. Cambridge University Press, 2018.

[22] A. P. Suppappola, *Applications in Time-Frequency Signal Processing*. CRC Press LLC, 2003.

[23] S. Chen, X. Dong, Z. Peng, W. Zhang, and G. Meng, "Nonlinear Chirp Mode Decomposition: A Variational Method," *IEEE Trans. Signal Process.*, vol. 65, no. 22, pp. 6024–6037, 2017.

[24] S. Sandoval and P. L. De Leon, "Recasting the (Synchrosqueezed) Short-Time Fourier Transform as an Instantaneous Spectrum," *Entropy*, vol. 24, no. 4, p. 518, 2022.

[25] S. Sandoval, H. Alshammari, M. Dalal, "ISA.jl: Instantaneous spectral Analysis in Julia," *SoftwareX*, 2022, in press. [Online]. Available: https://github.com/NMSU-ISA/ISA